

Design and Modal Analysis of Feedback Excitation Control System for Vertical Series Elastic Manipulator

Takatoshi Hondo and Ikuo Mizuuchi

Abstract—This paper describes a feedback excitation control system with consideration of gravity, which is a control method to obtain high kinetic energy by utilizing passive potential energy. In the case of a robot that has series elastic joints, peak kinetic energy becomes higher than that of a rigid robot with same motors. We have proposed the feedback excitation control for horizontal multiple-joint robots in our previous work. In this paper, we extend the feedback excitation control to systems that are affected by gravity, and we analyze the feedback excitation control system from the viewpoint of linear vibration mode. Validity of the proposed ‘coordinate or opposite phase controller’ is suggested by the modal analysis. We examine effective excitation controllers to utilize gravitational and elastic potential energy by simulations and experiments.

I. INTRODUCTION

The purpose of this research is to establish a motion control method utilizing passive elements such as elasticity, gravity and nonlinear dynamic properties of multiple-joint robot system. It is expected to realize a motion that does not depend only on actuator power by utilizing them. In the case of a robot that has series elastic elements[1] as shown in Fig.1, for example, speeds of links becomes instantaneously higher than that of a rigid robot with same motors[2], [3], [4]. This means that it is possible to obtain high kinetic energy by using low power driving systems and it is useful for “explosive” tasks in robots such as pitching and jumping.

Since Hogan’s research on mechanical impedance control [5], many researchers have been investigating utilization of mechanical elasticity ([1], [6], [7] etc.). Pioneering work on the utilization of elasticity for explosive motion in robots includes the 3D Hopper investigated by Raibert et al.[8]. High dynamic performance by a series elastic joint was investigated recently by the DLR group[2], [9], [10],

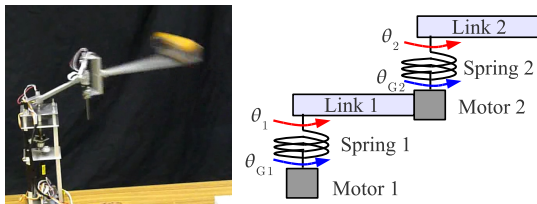


Fig. 1. Construction of a 2-joint series elastic manipulator

T. Hondo is with Department of Mechanical Systems Engineering, Tokyo University of Agriculture and Technology, hondo@mizuuchi.lab.tuat.ac.jp

I. Mizuuchi is with the Department of Mechanical Systems Engineering, Tokyo University of Agriculture and Technology, ikuo@mizuuchi.lab.tuat.ac.jp

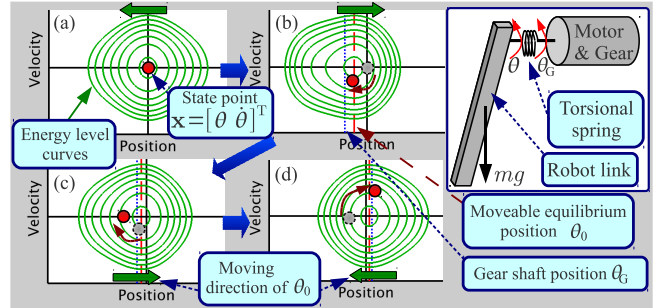


Fig. 2. Concept of feedback excitation control: resonance on a 1-joint series elastic system that is excited by a moveable equilibrium point

[11]. Control methods for obtaining high kinetic energy utilizing elasticity and gravity on multiple-joint robots that have nonlinear dynamics have not been discussed, however. Braun et al.[12] and Nakanishi et al.[13] discussed optimal variable stiffness control for explosive tasks with a 2-joint variable stiffness robot. This method needs a precise dynamic model and it is vulnerable to disturbance and variation in control objectives since this method depends on offline trajectory optimization. Ugurlu et al.[14] discussed a hopping trajectory generation method at resonance frequency. This method depends on, however, the experimental identification of resonance frequency, which may not be optimal frequency since resonance frequency of nonlinear systems depends on amplitude of state variables.

In our previous work[4], we proposed feedback excitation control and the excitation limit hypersurface to obtain high kinetic energy on multiple-joint series-elastic robots within joint limit ranges. It is difficult, however, to use this method for robots that is influenced by gravity since a horizontal robot is considered in [4]. Feedback excitation control should be extended to treat gravity. It is expected, in addition, to utilize not only elastic energy but also gravitational potential energy by taking gravity into consideration. In this paper, we examine 2 points as follows:

- Utilization of gravitational potential energy by feedback excitation control.
- Feasibility of higher kinetic energy amplification by synchronization of voltage command for each joint.

Feasibility of the control method is verified by simulations and ball throwing experiments.

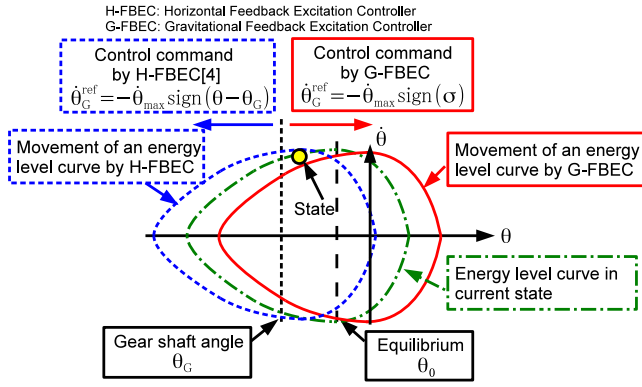


Fig. 3. Difference between horizontal and gravitational feedback excitation controllers: total energy is not increased by using the horizontal feedback excitation controller[4] when $\theta_G > \theta > \theta_0$ or $\theta_0 > \theta > \theta_G$.

II. FEEDBACK EXCITATION CONTROL WITH CONSIDERATION OF GRAVITY

A. Concept of Feedback Excitation Control: Resonance on Vibration System of Manipulator

Fig.2, right, shows a 1-joint series elastic robot that is excited by movement of equilibrium. Fig.2, left, shows energy level curves of the system in state space whose state variable is $\mathbf{x} = [\theta \ \dot{\theta}]^T$. θ is the link angle. We assume that the equilibrium point is not influenced by dynamic interaction from the spring. Here, we discuss energy transition of the system when the system is excited at the resonance frequency. When equilibrium $\mathbf{x}_0 = [\theta_0 \ 0]^T$ moves, energy level curves also move as shown in Fig.2. The relative position between the state point and energy level curves then changes.

Energy transition depends on link angle θ , the equilibrium position of the system θ_0 and the direction of the movement (or velocity) of the equilibrium position $\dot{\theta}_0$. When $\theta > \theta_0$, total energy increases if $\dot{\theta}_0 < 0$, and energy decreases if $\dot{\theta}_0 > 0$. When $\theta < \theta_0$, total energy increases if $\dot{\theta}_0 > 0$, and energy decreases if $\dot{\theta}_0 < 0$. By switching the moving velocity of the equilibrium position based on the relative position between θ and θ_0 , the equilibrium position moves in the resonance frequency when the system is linear. The resonance frequency or natural frequency cannot be defined for nonlinear dynamic systems such as a multiple-joint robot. By focusing on the energy increase, however, we obtain a feedback controller for nonlinear systems. In the case of an N -DOF manipulator, total energy increases by controlling the equilibrium position moving velocity of each joint $\dot{\theta}_{0i}$ based on the relative position of each joint $\theta_i - \theta_{0i}$ [4].

A resonance-based feedback controller was proposed by Uemura et al.[15], [16], [17] for robots that have parallel elastic joints. We propose a controller to be used for robots that have series elastic joints. The controller we propose can be used even for nonlinear spring joints as well.

B. Derivation of Feedback Excitation Controller with Consideration of Gravity

The feedback excitation controller for horizontal systems is derived by using energy integral of which anchoring

point is gear shaft angles θ_G since the equilibrium point of horizontal series elastic systems is always equal to gear shaft angles [4]. On vertical systems, however, the equilibrium position θ_0 is not equal to θ_G in general. Total energy of the vertical system is not always increased by using the horizontal feedback excitation controller as shown in Fig.3. Feedback excitation controllers for vertical systems should be derived by considering this point. In this section, we will derive them.

Equation of motion of an N -joint series elastic robot is described as

$$\mathbf{M}(\boldsymbol{\theta})\ddot{\boldsymbol{\theta}} + \mathbf{H}(\dot{\boldsymbol{\theta}}, \boldsymbol{\theta}) + \mathbf{G}(\boldsymbol{\theta}) + \mathbf{S}(\boldsymbol{\theta} - \boldsymbol{\theta}_G) = \mathbf{0}, \quad (1)$$

where $\boldsymbol{\theta} \in \mathbb{R}^{N \times 1}$ is the link angle vector, $\boldsymbol{\omega} = \dot{\boldsymbol{\theta}} \in \mathbb{R}^{N \times 1}$ is the link angular velocity vector, $\boldsymbol{\theta}_G \in \mathbb{R}^{N \times 1}$ is the gear shaft angle vector, $\mathbf{M}(\boldsymbol{\theta}) \in \mathbb{R}^{N \times N}$ is the inertial matrix of the link part, $\mathbf{H}(\boldsymbol{\theta}, \boldsymbol{\omega}) \in \mathbb{R}^{N \times 1}$ is the vector that describes centrifugal force and Coriolis force, $\mathbf{G}(\boldsymbol{\theta}) \in \mathbb{R}^{N \times 1}$ is the vector that describes gravity torque and $\mathbf{S}(\boldsymbol{\theta} - \boldsymbol{\theta}_G) \in \mathbb{R}^{N \times N}$ is the restoring torque vector of joint springs that has nonlinear characteristics in general. We obtain the following expression by multiplying $(\dot{\boldsymbol{\theta}} - \dot{\boldsymbol{\theta}}_0)^T$ from the left to (1).

$$\begin{aligned} & \dot{\boldsymbol{\theta}}^T \left\{ \mathbf{M}(\boldsymbol{\theta})\ddot{\boldsymbol{\theta}} + \mathbf{H}(\dot{\boldsymbol{\theta}}, \boldsymbol{\theta}) \right\} + (\dot{\boldsymbol{\theta}} - \dot{\boldsymbol{\theta}}_0)^T \left\{ \mathbf{G}(\boldsymbol{\theta}) + \mathbf{S}(\boldsymbol{\theta} - \boldsymbol{\theta}_G) \right\} \\ &= \dot{\boldsymbol{\theta}}_0^T \left\{ \mathbf{M}(\boldsymbol{\theta})\ddot{\boldsymbol{\theta}} + \mathbf{H}(\dot{\boldsymbol{\theta}}, \boldsymbol{\theta}) \right\} \end{aligned} \quad (2)$$

The following expression is derived by integrating (2) by time.

$$T + P = \int \left\{ \mathbf{M}(\boldsymbol{\theta})\ddot{\boldsymbol{\theta}} + \mathbf{H}(\dot{\boldsymbol{\theta}}, \boldsymbol{\theta}) \right\}^T \dot{\boldsymbol{\theta}}_0 dt + C \quad (3)$$

The first term of the left part of (3) T represents total kinetic energy of links as

$$T = \int \dot{\boldsymbol{\theta}}^T \left\{ \mathbf{M}(\boldsymbol{\theta})\ddot{\boldsymbol{\theta}} + \mathbf{H}(\dot{\boldsymbol{\theta}}, \boldsymbol{\theta}) \right\} dt. \quad (4)$$

(4) is derived by using passivity of the system. The second term P represents total potential energy, which is the integral of the second term of the left part of (2).

$$P = \int \left\{ \mathbf{G}(\boldsymbol{\eta} + \boldsymbol{\theta}_0) + \mathbf{S}(\boldsymbol{\eta} + \boldsymbol{\theta}_0 - \boldsymbol{\theta}_G) \right\}^T d\boldsymbol{\eta} \quad (5)$$

Here $\boldsymbol{\eta} = \boldsymbol{\theta} - \boldsymbol{\theta}_0$. Note that the relative angular velocity vector $\dot{\boldsymbol{\theta}} - \dot{\boldsymbol{\theta}}_0 (= \dot{\boldsymbol{\eta}})$ in (2) becomes $d\boldsymbol{\eta}$ in (5) by using the following variable transformation: $\dot{\boldsymbol{\eta}} dt = d\boldsymbol{\eta}$. Total potential energy P whose origin is $\boldsymbol{\theta} = \boldsymbol{\theta}_0$ ($\boldsymbol{\eta} = \mathbf{0}$) is derived by integrating total restoring torque $(\mathbf{G} + \mathbf{S})^T$ by $\boldsymbol{\eta}$ since restoring torque is $\mathbf{0}$ when $\boldsymbol{\eta} = \mathbf{0}$.

Because the left part of (3) represents the total mechanical energy and the right part represents the input energy, the integrand of the right part of (3) should be equal to or larger than 0 to constantly increase total energy of the system.

$$\left\{ \mathbf{M}(\boldsymbol{\theta})\ddot{\boldsymbol{\theta}} + \mathbf{H}(\dot{\boldsymbol{\theta}}, \boldsymbol{\theta}) \right\}^T \dot{\boldsymbol{\theta}}_0 \geq 0 \quad (6)$$

(6) is described by using restoring torque of the springs and gravity as shown below by using (1).

$$- \left\{ \mathbf{G}(\boldsymbol{\theta}) + \mathbf{S}(\boldsymbol{\theta} - \boldsymbol{\theta}_G) \right\}^T \dot{\boldsymbol{\theta}}_0 \geq 0 \quad (7)$$

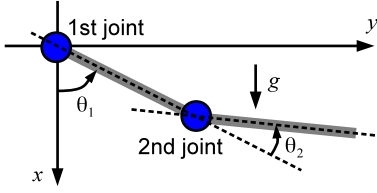


Fig. 4. Coordinate system of simulation model

(7) contains $\dot{\theta}_0$, which cannot be controlled directly. $\dot{\theta}_0$ is controlled by controlling $\dot{\theta}_G$. Relation between θ_0 and θ_G is described as

$$\mathbf{G}(\theta_0) + \mathbf{S}(\theta_0 - \theta_G) = \mathbf{0}. \quad (8)$$

Following expressions are derived by differentiating (8) by time.

$$\begin{aligned} \frac{\partial \mathbf{G}(\theta_0)}{\partial \theta_0} \dot{\theta}_0 + \frac{\partial \mathbf{S}(\theta_0 - \theta_G)}{\partial \theta_0} \dot{\theta}_0 - \frac{\partial \mathbf{S}(\theta_0 - \theta_G)}{\partial \theta_G} \dot{\theta}_G &= \mathbf{0} \\ \rightarrow (\Sigma_g + \Sigma_s) \dot{\theta}_0 &= \Sigma_s \dot{\theta}_G \end{aligned} \quad (9)$$

(7) can be described as follows by using (9).

$$-\{\mathbf{G}(\theta) + \mathbf{S}(\theta - \theta_G)\}^T (\Sigma_g + \Sigma_s)^{-1} \Sigma_s \dot{\theta}_G \geq 0 \quad (10)$$

Here, we introduce a vector as

$$\begin{aligned} \sigma^T &= \{\mathbf{G}(\theta) + \mathbf{S}(\theta - \theta_G)\}^T (\Sigma_g + \Sigma_s)^{-1} \Sigma_s \\ &= [\sigma_1 \quad \sigma_2 \quad \cdots \quad \sigma_i \quad \cdots \quad \sigma_N]. \end{aligned} \quad (11)$$

(10) is described by using the vector σ as

$$-\sum_{i=0}^N \sigma_i \dot{\theta}_{Gi} \geq 0. \quad (12)$$

The following expression is a sufficient condition for (10).

$$\dot{\theta}_{Gi}^{\text{ref}} = -\dot{\theta}_{\max i} \text{sign}(\sigma_i), \quad \forall i \quad (13)$$

$\dot{\theta}_{\max i}$ is the maximum gear shaft angular speed of the i -th joint. Total energy of the system always increases by controlling $\dot{\theta}_{Gi}$ based on (13). A velocity controller is needed to control gear shaft velocity. From the viewpoint of maximizing input power from the motors to the spring, however, it is desirable that the maximum voltage of the driving system E_{\max} is always applied to the motors. In this paper, the following controllers are used instead of the controllers (13).

$$E_i = -E_{\max} \text{sign}(\sigma_i), \quad \forall i \quad (14)$$

E_i is the voltage command for the i -th joint motor.

III. SIMULATIONS OF FEEDBACK EXCITATION CONTROL

A. Comparison between Horizontal and Vertical Systems

In this section, we evaluate kinetic energy increasing by using the controllers (14) in simulations. The simulation model is a 2-joint model that includes a motor mechanical and electrical dynamics as

$$\mathbf{R}\mathbf{I} + \mathbf{L}\dot{\mathbf{I}} + \mathbf{\Gamma}\mathbf{K}\dot{\theta}_G = \mathbf{E} \quad (15)$$

$$\mathbf{\Gamma}^2 \mathbf{J} \ddot{\theta}_G + \mathbf{\Gamma}^2 \mathbf{F} \dot{\theta}_G - \mathbf{S}(\theta - \theta_G) = \mathbf{\Gamma} \mathbf{K} \mathbf{I}. \quad (16)$$

TABLE I

SYSTEM PARAMETERS	
Parameter	value
ϕ_1	0.0155 [kgm ²]
ϕ_2	0.00392 [kgm ²]
ϕ_3	0.00338 [kgm ²]
g_1	0.880 [kgm ²]
g_2	0.241 [kgm ²]
$\mathbf{M}(\theta) =$	$\begin{bmatrix} \phi_1 + 2\phi_3 \cos \theta_2 & \phi_2 + \phi_3 \cos \theta_2 \\ \phi_2 + \phi_3 \cos \theta_2 & \phi_2 \end{bmatrix}$
$\mathbf{H}(\dot{\theta}, \theta) =$	$\begin{bmatrix} -\phi_3 \dot{\theta}_2 (2\dot{\theta}_1 + \dot{\theta}_2) \sin \theta_2 \\ \phi_3 \dot{\theta}_1^2 \sin \theta_2 \end{bmatrix}$
$\mathbf{G}(\theta) =$	$\begin{bmatrix} g_1 \sin \theta_1 + g_2 \sin(\theta_1 + \theta_2) \\ g_2 \sin(\theta_1 + \theta_2) \end{bmatrix}$

TABLE II

MOTOR PARAMETERS (MAXON RE16 4.5W)	
Parameter	Value
Resistance R_i	11.2[Ω]
Inductance L_i	4.52×10^{-4} [H]
Shaft inertia J_i	1.29×10^{-7} [kgm ²]
Torque constant K_i	1.62×10^{-2} [Nm/A]
Visco friction coef. F_i	2.28×10^{-7} [Nm · sec/rad]
Reduction ratio γ_i	157:1 (1st joint) 84:1 (2nd joint)

- $\mathbf{R} = \text{diag}(R_1, R_2, \dots, R_N)$: resistance matrix
- $\mathbf{L} = \text{diag}(L_1, L_2, \dots, L_N)$: inductance matrix
- $\mathbf{K} = \text{diag}(K_1, K_2, \dots, K_N)$: torque constant matrix
- $\mathbf{E} \in \mathcal{R}^{N \times 1}$: input voltage vector
- $\mathbf{I} \in \mathcal{R}^{N \times 1}$: motor current vector
- $\mathbf{J} = \text{diag}(J_1, J_2, \dots, J_N)$: rotor inertial matrix
- $\mathbf{F} = \text{diag}(F_1, F_2, \dots, F_N)$: viscous friction coef. matrix
- $\mathbf{\Gamma} = \text{diag}(\gamma_1, \gamma_2, \dots, \gamma_N)$: gear reduction ratio matrix

Coordinate system of the simulation model is shown in Fig.4. The link and motor parameters are shown in Table I and Table II respectively. The spring characteristics are linear whose spring constants are 0.492 [Nm/rad] in the simulations. The maximum input voltage E_{\max} is 7 [V]. The equilibrium angle vector θ_0 and σ are calculated by using Newton's method and Gaussian elimination.

Fig.5 shows kinetic energy transition in the simulation. Blue dotted curve indicates a result of the horizontal system with horizontal feedback excitation controller and an excitation limit hypersurface[4], black solid curve indicates a result of the vertical system with gravitational feedback excitation controller (14) and red chain curve indicates a result of the vertical system with the following controller.

$$E_1 = -E_{\max} \text{sign}(\sigma_1), \quad E_2 = -E_{\max} \text{sign}(\sigma_1) \quad (17)$$

In this paper, we call the controller (17) as the first joint reference controller. Peak kinetic energy of the vertical systems became larger than that of the horizontal system. The first joint reference controller (17) is the most effective in the three cases although (17) is not a sufficient condition for (10). We discuss a reason of this from the viewpoint of linear vibration mode in the next subsection.

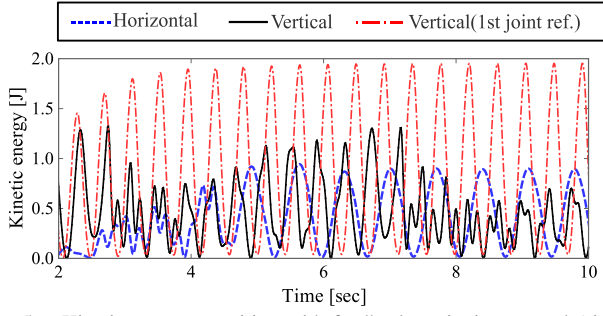


Fig. 5. Kinetic energy transition with feedback excitation control (simulation)

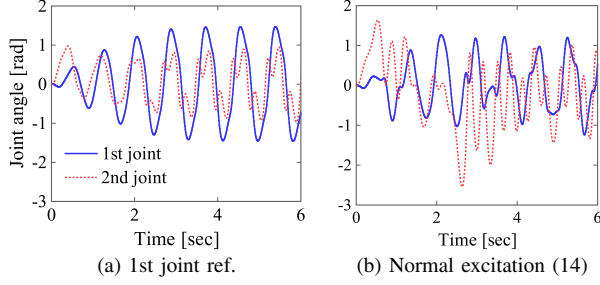


Fig. 6. Transition of joint angles of vertical systems (simulation)

B. Linearized System Analysis of First Joint Reference Control

Fig.6 shows transition of joint angles θ of vertical systems. Fig.6-(a) shows the result of the first joint reference controller (17) and Fig.6-(b) shows the result of the normal feedback excitation controller (14). Joint angles transition is almost cyclic and coordinate phase when the first joint reference controller is used as shown in the figure. We discuss this from the viewpoint of linear vibration mode. Following equation is a linear approximated system of (1) that is approximated around $\theta = \mathbf{0}$.

$$\mathbf{M}(\mathbf{0})\ddot{\theta} + \{\Sigma_g(\mathbf{0}) + \Sigma_s(\mathbf{0})\}(\theta - \theta_0) \approx \mathbf{0} \quad (18)$$

(18) is decoupled by using a diagonalization matrix $\mathbf{P} \in \mathbb{R}^{N \times N}$.

$$\ddot{\xi} + \Lambda(\xi - \xi_0) \approx \mathbf{0} \quad (19)$$

$\xi = \mathbf{P}^{-1}\theta$ and $\xi_0 = \mathbf{P}^{-1}\theta_0$ are modal variable vectors and $\Lambda = \mathbf{P}^{-1}\mathbf{M}(\mathbf{0})^{-1}\{\Sigma_g(\mathbf{0}) + \Sigma_s(\mathbf{0})\}\mathbf{P} = \text{diag}(\lambda_1, \lambda_2, \dots, \lambda_N)$ is an eigenvalue matrix. (19) is described as individual differential equations of each modal variable ξ_i as

$$\ddot{\xi}_i + \lambda_i(\xi_i - \xi_{0i}) \approx 0. \quad (20)$$

An N -joint system has N modes. Here, we define the first mode as the mode that has the most small eigenvalue $\lambda_1 < \lambda_i, \forall i \neq 1$. The first mode describes a coordinate phase transition component of joint angle and angular velocity of all joints. Energy increase condition is described by using modal variables as

$$-\dot{\xi}_0^T \Lambda(\xi - \xi_0) \geq 0. \quad (21)$$

Here, we focus on the first mode energy.

$$-\dot{\xi}_{10} \lambda_1 (\xi_1 - \xi_{10}) \leq 0 \quad (22)$$

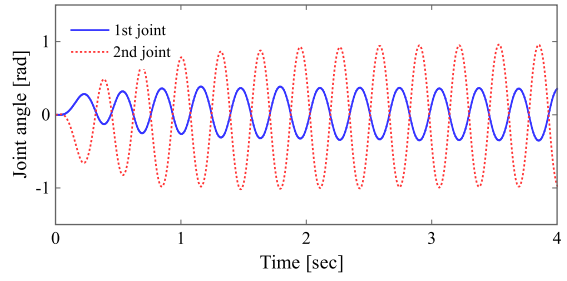


Fig. 7. Second mode excitation by using opposite phase controller (28)

Equilibrium position moving velocity of the modal space $\dot{\xi}_{10}$ is described by using that of the joint space $\dot{\theta}_0$ as

$$\dot{\xi}_{10} = \dot{\theta}_0^T \mathbf{p}_1, \quad \mathbf{p}_1 = [p_{11} \ p_{12} \ \dots \ p_{1N}]^T \quad (23)$$

where $[p_1 \ p_2 \ \dots \ p_N] = \mathbf{P}^{-1}$. (23) is described using $\dot{\theta}_G$.

$$-\dot{\theta}_G^T \Psi \mathbf{p}_1 \lambda_1 (\xi_1 - \xi_{10}) \geq 0 \quad (24)$$

$$\Psi = \Sigma_s^T(\mathbf{0}) \{(\Sigma_g(\mathbf{0}) + \Sigma_s(\mathbf{0}))^{-1}\}^T = \{\psi_{ij}\} \quad (25)$$

Voltage commands E_1 and E_2 for 2-joint system are described as follows similar to (14).

$$E_1 = -E_{\max} \text{sign}\{\lambda_1(\psi_{11}p_{11} + \psi_{12}p_{12})(\xi_1 - \xi_{10})\} \quad (26)$$

$$E_2 = -E_{\max} \text{sign}\{\lambda_1(\psi_{21}p_{11} + \psi_{22}p_{12})(\xi_1 - \xi_{10})\} \quad (27)$$

λ_1, ψ_{ij} and p_{ij} are constants since the linearized system is considered. This means that voltage commands for all joints are decided by the same variable $\xi_1 - \xi_{10}$, and the first mode vibration is excited by this controller. The voltage command transition of each joint becomes coordinate phase or opposite phase transition in accordance with a sign of $\psi_{11}p_{11} + \psi_{12}p_{12}$ and $\psi_{21}p_{11} + \psi_{22}p_{12}$. They are calculated as follows by using parameters shown in Table I.

$$\psi_{11}p_{11} + \psi_{12}p_{12} = -0.269$$

$$\psi_{21}p_{11} + \psi_{22}p_{12} = -0.140$$

In this case, the first mode vibration is excited by coordinate phase controllers.

On 2-joint robots whose joint axes are parallel, kinetic energy becomes large when angular velocity of all joints are same sign compared with opposite sign if the absolute angular speeds are the same, and the first joint reference controller, which is a coordinate phase controller, generate higher kinetic energy than that of normal excitation controller, which is a coordinate and opposite phase combined controller. We have discussed the linearized system (18) and this is not a strict discussion, and (17) does not always satisfy the energy increasing condition (6). Energy loss phase would be included by using (17), and it is needed to the energy loss is sufficiently small to obtain a kinetic energy amplification.

The simulation results show that, however, the direction of the linear modal analysis may be useful. For example, the second mode vibration is excited by an opposite phase controller as follows according to the same analysis as shown in Fig.7.

$$E_1 = -E_{\max} \text{sign}(\sigma_1), \quad E_2 = -E_{\max} \text{sign}(-\sigma_1) \quad (28)$$

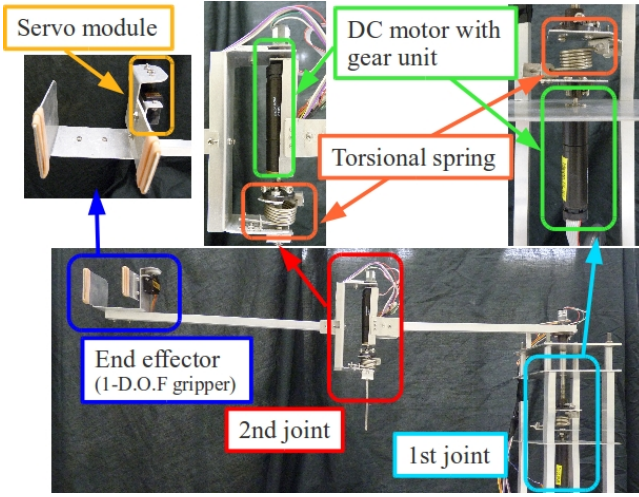


Fig. 8. Overview of experimental setup

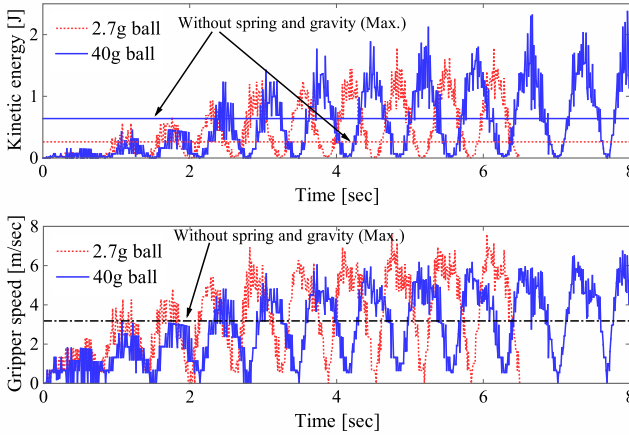


Fig. 9. Kinetic energy and gripper speed transition with feedback excitation control (experiment)

Vibration mode switching would be important when a specific task is considered. For example, the first mode vibration is useful for ball throwing motion. The first mode vibration contributes not only the kinetic energy amplification but also the end-tip speed amplification as shown in experiments in the next section. On the other hand, second mode vibration would be important for motions such as jumping.

IV. BALL THROWING EXPERIMENTS ON 2-JOINT SERIES ELASTIC ROBOT

This section describes pitching motion experiment as an application of feedback excitation control on the 2-joint series elastic robot as shown in Fig.8. This robot has a 1DOF gripper as the end effector. We tested 2 cases of different mass of the throwing object: 2.7 [g] and 40 [g]. Maximum input voltage E_{\max} is 7 [V]. The controller is the first joint reference controller (17), which is the most effective controller in simulations shown in Fig.5.

Fig.9 shows kinetic energy and gripper speed transition in the experiments. Red dotted curves indicate results of 2.7 [g] ball throwing and blue solid curves indicate results of

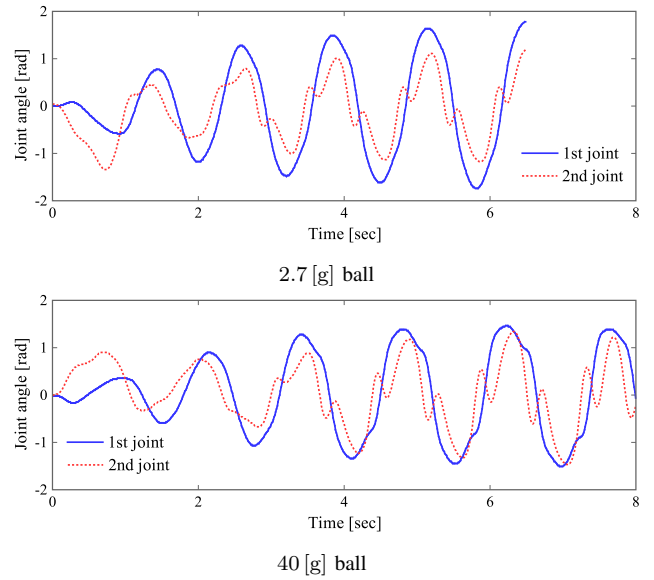


Fig. 10. Joint angle transition in experiments

40 [g] ball throwing. Kinetic energy shown in Fig.9 is sum of links and pitching object kinetic energy. Maximum kinetic energy T_{rigid} and gripper speed v_{rigid} without any springs and gravity are also indicated in Fig.9. They are described as

$$T_{\text{rigid}} = \frac{1}{2} \boldsymbol{\omega}_{\infty}^T \mathbf{M}(\mathbf{0}) \boldsymbol{\omega}_{\infty} \quad (29)$$

$$v_{\text{rigid}} = \sqrt{\boldsymbol{\omega}_{\infty}^T \mathbf{J}(\mathbf{0})^T \mathbf{J}(\mathbf{0}) \boldsymbol{\omega}_{\infty}}, \quad \boldsymbol{\omega}_{\infty} = [\omega_{\infty 1} \quad \omega_{\infty 2}]^T \quad (30)$$

$\omega_{\infty i}$ ($i = 1, 2$) is steady-state angular speed of the i -th joint gear shaft and $\mathbf{J}(\boldsymbol{\theta})$ is a Jacobian matrix between the joint angles and position of the gripper. Maximum kinetic energy and gripper speed became larger than that of rigid cases T_{rigid} and v_{rigid} . Maximum kinetic energy became about 4.5 times larger than T_{rigid} and maximum gripper speed became about 2 times larger than v_{rigid} on 2.7 [g] ball throwing. Fig.10 shows the joint angle transition in experiments. Coordinate phase vibration is excited by the first joint reference controller as shown in Fig.10 similar to the simulations. Fig.11 shows a sequential photographs of the ball throwing experiment.

V. CONCLUSIONS

In this paper, we have proposed feedback excitation control with consideration of gravity, which is a control method to obtain high kinetic energy utilizing gravitational and elastic potential energy. Kinetic energy amplification by the control method have been verified by simulations and experiments. In addition, we have examined higher kinetic energy amplification by using first joint reference control than the normal excitation. It is suggested that linear first or second vibration modes are excited by coordinate or opposite phase controllers. Vibration mode switching is important when a specific tasks is considered, and there is a possibility of adaptive control for various control objectives in “explosive” tasks of multiple-joint series-elastic robots.

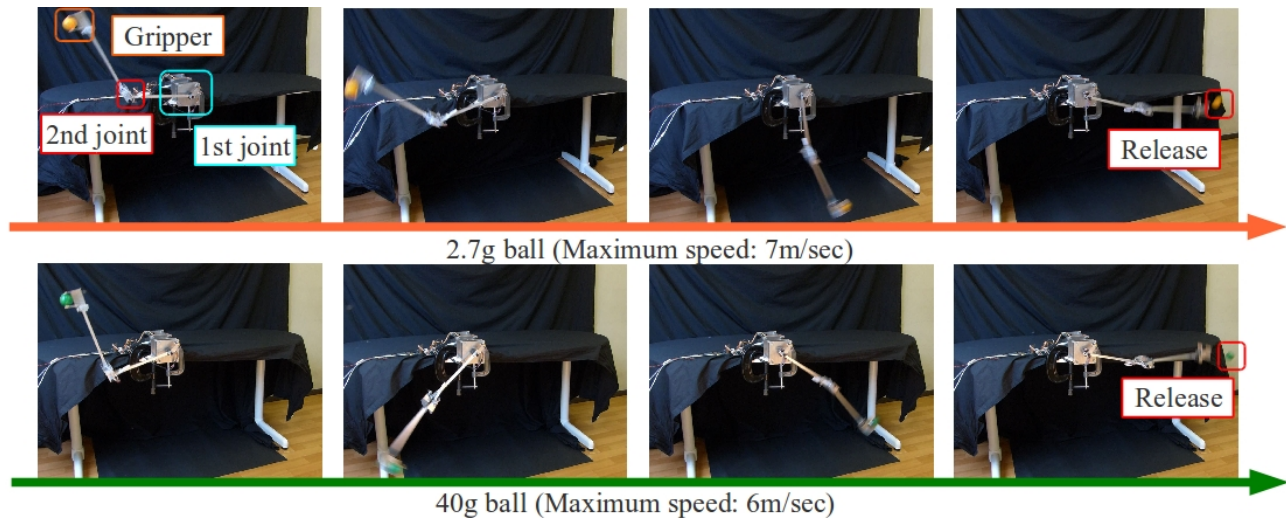


Fig. 11. Sequential photographs of ball throwing motions with feedback excitation control

Feasibility of the control method has been evaluated in experiments. Maximum kinetic energy became about 4 times larger than that of a rigid robot with the same motors and links.

Extending the modal analysis for nonlinear systems is a future work. Extending the feedback excitation control for legged mobile robots and application to jumping and running motions is also a future work. Kinetic energy amplification is useful for these motions too. Establishing a control method with consideration of balancing and landing is, however, left to a future work. Establishing a feedback excitation control method for variable stiffness joints is also a future work.

ACKNOWLEDGEMENTS

This work was supported by a JSPS KAKENHI Grant Number K100243085 (Grant-in-Aid for JSPS Fellows).

REFERENCES

- [1] G. A. Pratt and M. M. Williamson. Series elastic actuators. In *Proceedings of the 1995 IEEE/RSJ International Conference on Intelligent Robots and Systems*, pages 399–406, 1995.
- [2] S. Haddadin, T. Laue, U. Frese, S. Wolf, A. Albu-Schäffer, and G. Hirzinger. Kick it with elasticity: Safety and performance in humanoid soccer. *Robotics and Autonomous Systems (RAS): Special Issue on Humanoid Soccer Robots*, 57(8):761–775, 2009.
- [3] T. Hondo and I. Mizuuchi. Analysis of the 1-Joint Spring-Motor Coupling System and Optimization Criteria Focusing on the Velocity Increasing Effect. In *Proceedings of the 2011 IEEE International Conference on Robotics & Automation*, pages 1412–1418, 2011.
- [4] T. Hondo and I. Mizuuchi. Kinetic energy maximization on elastic joint robots based on feedback excitation control and excitation limit hypersurface. *Journal of Robotics and Mechatronics*, 35(2), 2013.
- [5] N. Hogan. Adaptive control of mechanical impedance by coactivation of antagonist muscles. *IEEE Transactions on Automatic Control*, AC-29(8):681–690, 1984.
- [6] I. Mizuuchi, Y. Nakanishi, Y. Sodeyama, Y. Namiki, T. Nishino, N. Muramatsu, J. Urata, K. Hongo, T. Yoshikai, and M. Inaba. An advanced musculoskeletal humanoid kojiro. In *2007 7th IEEE-RAS International Conference on Humanoid Robots*, pages 294–299, 29 2007-dec. 1 2007.
- [7] R. Niiyama, K. Kakitani, and Y. Kuniyoshi. Learning to jump with a musculoskeletal robot using a sparse coding of activation. In *Proceedings of the IEEE International Conference on Robotics & Automation 2009 Workshop on Approaches to Sensorimotor Learning on Humanoid Robots*, pages 30–31, Kobe, Japan, May 2009.
- [8] M. H. Raibert, H. B. B. Jr., and M. Chepponis. Experiments in balance with a 3d one-legged hopping machine. *The International Journal of Robotics Research*, 3:75–92, 2012.
- [9] O. Eiberger, S. Haddadin, M. Weis, A. Albu-Schäffer, and G. Hirzinger. On Joint Design with Intrinsic Variable Compliance: Derivation of the DLR QA-Joint. In *Proceedings of the 2010 IEEE International Conference on Robotics & Automation*, pages 1687–1694, 2010.
- [10] F. Petit, M. Chalon, W. Friedl, M. Grebenstein, A. Albu-Schäffer, and G. Hirzinger. Bidirectional Antagonistic Variable Stiffness Actuation: Analysis, Design & Implementation. In *Proceedings of the 2010 IEEE International Conference on Robotics & Automation*, pages 4189–4196, 2010.
- [11] S. Haddadin, M. Weis, S. Wolf, and A. Albu-Schäffer. Optimal Control for Maximizing Link Velocity of Robotic Variable Stiffness Joints. In *Proceedings of the International Federation of Automatic Control*, pages 6863–6871, 2011.
- [12] D. Braun, M. Howard, and S. Vijayakumar. Optimal variable stiffness control: formulation and application to explosive movement tasks. *Autonomous Robots*, 33:237–253, 2012.
- [13] J. Nakanishi and S. Vijayakumar. Exploiting Passive Dynamics with Variable Stiffness Actuation in Robot Brachiation. In *Proceedings of the 2012 Robotics: Science and Systems Conference*, 2012.
- [14] B. Ugurlu, J. Saglia, N. Tsagarakis, and D. Caldwell. Hopping at the resonance frequency: A trajectory generation technique for bipedal robots with elastic joints. In *Robotics and Automation (ICRA), 2012 IEEE International Conference on*, pages 1436–1443, may 2012.
- [15] M. Uemura, K. Kanaoka, and S. Kawamura. A New Control Method Utilizing Stiffness Adjustment of Mechanical Elastic Elements for Serial Link Systems. In *Proceedings of the 2007 IEEE International Conference on Robotics & Automation*, pages 1437–1442, 2007.
- [16] M. Uemura, K. Kimura, and S. Kawamura. Generation of energy saving motion for biped walking robot through resonance-based control method. In *Proceedings of the 2009 IEEE/RSJ International Conference on Intelligent Robots and Systems*, pages 2928–2933, 2009.
- [17] M. Uemura, H. Oono, H. Goya, and S. Kawamura. Control Strategy for Continuous Jumping of Legged Robot Utilizing Resonance. In *The 13th International Conference on Climbing and Walking Robots and Support Technologies for Mobile Machines (CLAWAR2010)*, pages 1153–1160, 2010.